Mean-field theory of polynuclear surface growth

1998 J. Phys. A: Math. Gen. 31 5001

(http://iopscience.iop.org/0305-4470/31/22/005)

J. Phys. A: Math. Gen. **31** (1998) 5001–5012. Printed in the UK PII: S0305-4470(98)89828-4

Mean-field theory of polynuclear surface growth

E Ben-Naim†, A R Bishop†, I Daruka†‡ and P L Krapivsky§

† Theoretical Division and Center for Nonlinear Studies, Los Alamos National Laboratory, Los Alamos, NM 87545, USA

‡ Department of Physics, University of Notre Dame, Notre Dame, IN 46556, USA

§ Center for Polymer Studies and Department of Physics, Boston University, Boston, MA 02215, USA

Received 8 December 1997, in final form 2 March 1998

Abstract. We study statistical properties of a continuum model of polynuclear surface growth on an infinite substrate. We develop a self-consistent mean-field theory which is solved to deduce the growth velocity and the extremal behaviour of the coverage. Numerical simulations show that this theory gives an improved approximation for the coverage compared to the previous linear recursion relations approach. Furthermore, these two approximations provide useful upper and lower bounds for a number of characteristics including the coverage, growth velocity and the width exponent.

1. Introduction

Kinetics of surface growth is a fascinating field that has been the subject of intense current research [1–4]. It is well established that as the surface grows its morphology remains scale invariant, and for example, fluctuations in the interface height exhibit an asymptotic scaling behaviour. While the understanding of growth on one-dimensional (1D) substrates is rather comprehensive, in the physical case of two-dimensional substrates current theoretical understanding remains incomplete [3, 4].

In this study we focus on an appealingly simple yet non-trivial surface growth problem, the so-called polynuclear growth (PNG) model [5–7]. The PNG model describes the evolution of islands that nucleate at random on top of previously nucleated islands and grow in a radial direction. This model is appropriate for describing situations where there is a competition between growth along the step edges and growth due to nucleation, as is the case in polymer crystal growth [8, 9].

The submonolayer version of the PNG model is identical to the classical Kolmogorov–Avrami–Johnson–Mehl (KAJM) nucleation-and-growth process [10–12], where exact results for the coverage and more detailed statistical properties are possible [13–16]. Using the exact solution for the KAJM coverage, an approximate linear recursion relations (LRR) approach to the PNG process in arbitrary dimension was suggested [6, 17–19].

In one dimension, the PNG model is equivalent to an ensemble of 'kinks' (down steps) and 'antikinks' (up steps) moving ballistically and annihilating upon collision. Steady states on finite 1D substrates were obtained analytically using the fact that kinks (antikinks) are uncorrelated [5, 20, 21]. In the steady state, the width scales with system size L according to $w(L) \sim \sqrt{L}$, i.e. the roughness exponent is $\chi = \frac{1}{2}$. However, the non-equilibrium behaviour and especially the asymptotic time dependence remains an open problem, despite a number of studies [18–24].

0305-4470/98/225001+12$19.50

Our goal is to develop a self-consistent approach that can be viewed as a mean-field theory (MFT) of the PNG process, and to compare it with the previous LRR approximation as well as with numerical simulations. We shall show that MFT offers a better description for the time-dependent coverage, and that the two approaches, when combined, provide upper and lower bounds for the coverage and the growth velocity.

This paper is organized as follows. In section 2 we define the PNG model. In section 3, we develop a self-consistent mean-field approximation; we find that possible growth velocities are bounded from below, $v \geqslant v_{\min}$, showing that the minimal velocity is actually selected. We also solve the coverage profile in the tail regions. In section 4, we review the LRR approach and derive the coverage profile analytically. In section 5, we present simulation results, with our conclusions given in section 6.

2. The PNG Model

The PNG is a continuous time, off-lattice model which contains both deterministic and stochastic events. Starting from a flat uniform d-dimensional substrate at time $t = 0$, seeds of negligible size nucleate at random times and random positions at a constant rate per unit area. Once created, islands grow laterally at a constant velocity in the radial direction. When two islands in the same layer meet they coalesce, and the joint perimeter continues to grow in the corresponding radial direction. Meanwhile, nucleation continuously generates additional layers on top of previously nucleated layers. Clearly, there are no overhangs in this model, a feature which considerably simplifies the analysis. Another important simplification in the PNG model is that the nucleation rate is uniform in time as well as in space, i.e. it is independent of the local surface structure. Without loss of generality, we set the nucleation rate and the radial growth velocity to unity. This can be achieved by an appropriate rescaling of space and time.

Below, we concentrate on $S_j(t)$, the uncovered fraction in the jth layer at time t. This important characteristic of multilayer growth gives the net exposed fraction of the jth layer, $S_j(t) - S_{j-1}(t)$, and can therefore be used to calculate relevant statistical properties. The variable j plays the role of the local height h, often used in surface growth studies. In general $\langle f(j)\rangle = \sum_{j=0}^{\infty} f(j)[S_{j+1}(t) - S_j(t)]$, and in particular the average height is given by

$$h(t) = \langle j\rangle = \sum_{j=1}^{\infty} j[S_{j+1}(t) - S_j(t)]. \tag{1}$$

Fluctuations in the height are quantified by the mean square width $w^2(t)$ defined via

$$w^2(t) = \langle j^2\rangle - \langle j\rangle^2 = \sum_{j=1}^{\infty} j^2[S_{j+1}(t) - S_j(t)] - h^2(t). \tag{2}$$

We expect a linear growth in time for the average height, $h(t) \simeq vt$, and an algebraic growth of the width, $w(t) \sim t^{\beta}$, with *a priori* unknown width exponent β. In other words, the uncovered fraction obeys the following wavelike form

$$S_j(t) = F\left(\frac{j - vt}{t^{\beta}}\right). \tag{3}$$

The argument reflects the overall shift in the position of the wavefront, and the multiplicative scale accounts for the algebraic widening of the front. This expression also serves as a definition of the width exponent β, which is equivalent to equation (2).

Away from the front region, we anticipate the following extremal behaviour of the scaling function $F(z)$:

$$F(z) \sim \begin{cases} 1 - \exp(-z^{\sigma_+}) & z \to \infty \\ \exp(-|z|^{\sigma_-}) & z \to -\infty. \end{cases} \tag{4}$$

Thus the exponents $\sigma_\pm$ characterize relaxation away from the front region [25]. The exponent σ_+ which describes large positive fluctuations in the height can simply be related to the roughness exponent. Consider a large positive height fluctuation, $j = Avt$, with $A \gg 1$. Such large 'towers' can be only created by an anomalously large number, Avt, of nucleation events localized in the same region. Given the Poisson nature of the nucleation events, such fluctuations are suppressed exponentially. Thus, the quantity $1 - S_{Avt}(t)$ is estimated by $\exp(-t)$, but since equation (4) gives $\exp[-t^{\sigma_+(1-\beta)}]$, we conclude that

$$\sigma_+ = \frac{1}{1-\beta}. \tag{5}$$

In this study, we focus on systems with infinite lateral size. If the size is finite, it eventually becomes important and the width follows the scaling form $w(t, L) \sim L^\chi \mathcal{W}(t/L^z)$. The infinite size limit corresponds to $t \ll L^z$ where the size dependence disappears and therefore $w(t) \sim t^\beta$ with $\beta = \chi/z$ follows [3].

3. Mean-field theory

3.1. One dimension

We start with the PNG model in one dimension where a more comprehensive analysis is possible. In this situation, steps nucleate in pairs and move away from each other with a constant velocity. The constant nucleation rate and the growth velocity are set to unity, without loss of generality. Hence, the length of an island at time t after birth equals $2t$. Consider $f_j(x, t)$, the density of gaps of length x at time t in the jth layer. This distribution evolves according to

$$\frac{\partial f_j(x,t)}{\partial t} = 2\frac{\partial f_j(x,t)}{\partial x} + \gamma_j(t)\left[-x f_j(x,t) + 2\int_x^\infty dy\, f_j(y,t)\right]. \tag{6}$$

The spatial derivative term describes the shrinkage of gaps. The last two terms account for changes due to nucleation and thus, are proportional to the overall nucleation rate at the jth layer, $\gamma_j(t)$. The loss term is proportional to the gap length and the gain term describes creation of gaps from larger gaps.

Equations (6) contain yet unknown nucleation rates $\gamma_j(t)$ which will be chosen to satisfy the correct kinetic equations for the uncovered fractions

$$S_j(t) = \int_0^\infty dx\, x f_j(x,t) \tag{7}$$

and the gap (or island) densities

$$N_j(t) = \int_0^\infty dx\, f_j(x,t). \tag{8}$$

The uncovered fraction decreases with a rate proportional to the island density, $\dot{S}_j(t) = -2N_j(t)$, and by integrating equations (6) we recover this exact equation. The island density changes owing to the disappearance of gaps and to nucleation. The total nucleation rate is proportional to the exposed fraction of the jth layer and thus, $\dot{N}_j(t) =$

$-2f_j(0,t) + S_j(t) - S_{j-1}(t)$. On the other hand, by integrating equations (6) we obtain $\dot{N}_j(t) = -2f_j(0,t) + \gamma_j(t)S_j(t)$. Therefore, the choice

$$\gamma_j(t) = 1 - \frac{S_{j-1}(t)}{S_j(t)} \tag{9}$$

guarantees that the gap density evolves according to the *exact* rate equation. The expression of equation (9) for the nucleation rate $\gamma_j(t)$ in the jth layer is intuitively appealing since the total unit nucleation rate should be reduced to account for nucleation events below the jth layer. Taking into account that $S_0(t) \equiv 0$ we find $\gamma_1(t) \equiv 1$ and we note that equation (6) for the first layer agrees with the exact KAJM equation [13]. Thus, the set of rate equations (6) with the nucleation rates (9) provides a self-consistent description of the 1D PNG model. It is exact for the first layer, and additionally, the first two moments of the gap density satisfy the correct rate equations. However, it is a mean-field description since it assumes a spatially homogeneous nucleation rate $\gamma_j(t)$.

The gap density is found to be exponential, and the formal solution reads

$$f_j(x,t) = g_j^2(t) \exp\left[- g_j(t)x - 2\int_0^t d\tau\, g_j(\tau) \right] \tag{10}$$

with $g_j(t) = \int_0^t d\tau\, \gamma_j(\tau)$. The uncovered fraction and the island density are evaluated using equations (7) and (8):

$$\begin{aligned} S_j(t) &= \mathrm{e}^{-2\int_0^t d\tau\, g_j(\tau)} \\ N_j(t) &= g_j(t)S_j(t). \end{aligned} \tag{11}$$

Evaluating $d^2 \ln S_j(t)/dt^2$ together with equation (9) and $\dot{g}_j(t) = \gamma_j(t)$, leads to an infinite set of recursive differential equations for the uncovered fraction

$$\ddot{S}_j - \dot{S}_j^2 S_j^{-1} + 2(S_j - S_{j-1}) = 0. \tag{12}$$

Equations (12) should be solved subject to the initial conditions $S_j(0) = 1$ and $\dot{S}_j(0) = 0$ for $j \geqslant 1$. The recursive structure of equations (12) reflects the fact that the kinetics of a given layer is *unrelated* to that of all the above layers (owing to the absence of overhangs). Additionally, equations (12) agree with the nature of the PNG model implying that the kinetics of a given layer should be *directly* coupled only to the previous layer.

Using $S_0(t) \equiv 0$, $S_1(t)$ is determined, then $S_2(t)$, etc. Thus, for the first layer, the KAJM nucleation-and-growth results are reproduced [13]

$$\begin{aligned} S_1(t) &= \mathrm{e}^{-t^2} \\ f_1(x,t) &= t^2 \mathrm{e}^{-xt-t^2}. \end{aligned} \tag{13}$$

It is also possible to solve analytically for the second layer

$$\begin{aligned} S_2(t) &= \cosh^2 t\, \mathrm{e}^{-t^2} \\ f_2(x,t) &= [t\cosh t - \sinh t]^2 \mathrm{e}^{-(t-\tanh t)x-t^2}. \end{aligned} \tag{14}$$

Using the transformation, $S_j(t) = \exp[u_j(t) - t^2]$, the differential equations (12) formally simplify to a directed version of the Toda equations [26], $\ddot{u}_j = 2\exp[u_{j-1} - u_j]$, with the initial conditions $u_j(0) = \dot{u}_j(0) = 0$ and the boundary condition $u_1(t) = 0$. Despite this simplification it is not possible to integrate these equations, and we solve numerically for $S_j(t)$. Figure 1 shows how the coverage in a given layer changes with time. We note that the coverage quickly relaxes onto a travelling wave form with a finite width, $S_j(t) \to F(j - vt)$.

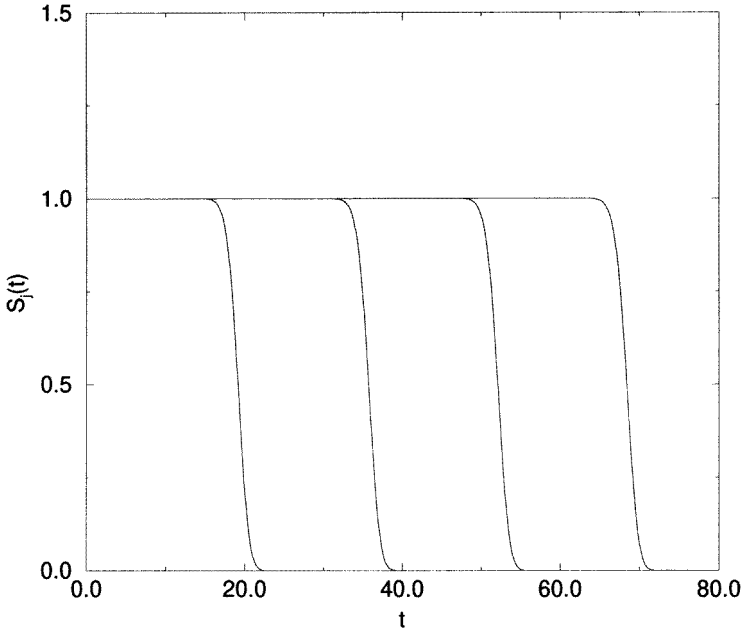

Figure 1. The uncovered fraction $S_j(t)$ versus time for layers $j = 20$, 40, 60 and 80. Clearly, the coverage follows a travelling waveform.

Some quantitative characteristics of the travelling wave can be determined analytically. For $j - vt \gg 1$, the nonlinear term in (12) is negligible and equations (12) become linear. Thus, we write

$$1 - S_j(t) \sim \mathrm{e}^{-\alpha(j-vt)} \qquad j - vt \gg 1 \tag{15}$$

with a yet unknown coefficient α. Substituting into equations (12) gives

$$v^2 = 2\frac{\mathrm{e}^{\alpha} - 1}{\alpha^2}. \tag{16}$$

The right-hand side has a minimum at $\alpha = 1.593\,62$. Therefore any velocity in the interval $[v_{\min}, \infty)$ with $v_{\min} = 1.757\,35$ is possible. Our numerical integration shows a velocity that falls within 0.1% of $v_{\min}$, thereby implying that the minimal velocity is selected. Such minimum velocity selection is ubiquitous and occurs for a wide class of initial conditions [27, 28].

To obtain the asymptotic behaviour in the other extreme, $z = j - vt \to -\infty$, we first note that $S_2(t) \gg S_1(t)$, as follows from (13) and (14). We assume this for all layers behind the front; we will check this assumption $S_j(t) \gg S_{j-1}(t)$ *a posteriori*. This reduces equations (12) to $\ddot{S}_j - \dot{S}_j^2 S_j^{-1} + 2S_j = 0$ which is solved to yield $S_j(t) = \exp(-t^2 + A_j t + B_j)$. The travelling wave form implies that $S_j(t)$ should be a function of a single variable $z = j - vt$. This determines the constants A_j and B_j, and we find $S_j(t) = F(z) \sim \exp(-z^2/v^2)$. One can verify that the assumption $S_j(t) \gg S_{j-1}(t)$ is valid.

3.2. Arbitrary dimension

The above analysis cannot be generalized in a straightforward manner to $d \neq 1$ since the gap distribution is intrinsically one-dimensional. However, it is still possible to obtain a

mean-field description for the uncovered fraction.

Consider a KAJM nucleation-and-growth process where the rate of nucleation events $\gamma(t)$ is homogeneous in space but time dependent. Ignoring the overlap between growing disks, the uncovered fraction $S(t)$ decreases with time according to

$$\frac{dS(t)}{dt} = -d\Omega_d \int_0^t d\tau\, \gamma(\tau)(t-\tau)^{d-1} \tag{17}$$

where $\Omega_d = \pi^{d/2}/\,\Gamma(1+d/2)$ is the volume of the d-dimensional unit sphere and $d\Omega_d$ is its surface area [29] (Γ is the gamma function). Thus, equation (17) overestimates the decay rate since some of the area is already covered. Nevertheless, this may be corrected if $(-dS/dt)$ is reduced by the uncovered fraction, S,

$$\frac{dS(t)}{dt} = -d\Omega_d\, S(t) \int_0^t d\tau\, \gamma(\tau)(t-\tau)^{d-1}. \tag{18}$$

For a constant nucleation rate, $\gamma = 1$, equation (18) gives

$$S(t) = \exp\left[-\frac{\Omega_d t^{d+1}}{d+1}\right]. \tag{19}$$

Thus, the exact KAJM coverage is recovered. Furthermore, a generalization of the KAJM solution to time-dependent nucleation rates appears to be equivalent to equation (18) [14].

We now return to the PNG model. Note that the non-local in time integro-differential equation (18) can be converted to a higher-order ordinary differential equation $d^{d+1}\ln S_j(t)/dt^{d+1} = -d!\,\Omega_d\gamma_j(t)$. Unlike the 1D case, it is not possible to derive the nucleation rate self-consistently. However, assuming a spatially homogeneous nucleation rate [7] implies the total nucleation rate $\gamma_j(t)S_j(t) = S_j(t) - S_{j-1}(t)$ and therefore equation (9). Thus we arrive at the following generalization of the mean-field equation (12) for the uncovered fraction

$$\frac{d^{d+1}}{dt^{d+1}}\,\ln S_j + d!\,\Omega_d\left[1 - \frac{S_{j-1}(t)}{S_j(t)}\right] = 0. \tag{20}$$

The analysis presented in the one-dimensional case applies for arbitrary dimensions. For example, the transformation $S_j(t) = \exp[u_j(t) - \Omega_d t^{d+1}/(d+1)]$ reduces equations (20) to a set of generalized directed Toda equations $d^{d+1}u_j/dt^{d+1} = d!\Omega_d \exp[u_{j-1} - u_j]$. Analysis of these equations or equations (20) reveals that the coverage relaxes to a travelling wave with a finite width. To determine the growth velocity, we insert the ansatz of equation (15) into equations (20) to find

$$v^{d+1} = d!\Omega_d \frac{\mathrm{e}^{\alpha} - 1}{\alpha^{d+1}}. \tag{21}$$

This provides the lower bound for the growth velocity, $v_d \geqslant v_d^{\min}$. Again the minimal velocity should be selected, and for example $v_0 = 1$, $v_1 = 1.757\,35$, $v_2 = 1.671\,15$, and $v_d \simeq \sqrt{2\pi e/d}$ when $d \to \infty$. Furthermore, in finite dimensions MFT predicts universal exponents $\beta = 0$, $\sigma_+ = 1$, and $\sigma_- = 2$. (Note that the relationship of equation (5) is obeyed.)

In the zero-dimension limit, the behaviour changes qualitatively. Indeed, for the $d = 0$ case equations (20) become *linear*,

$$\frac{dS_j}{dt} + S_j = S_{j-1}. \tag{22}$$

Solving (22) recursively yields the uncovered fraction, $S_j(t) = \mathrm{e}^{-t}\sum_{i=0}^{j-1} t^i/i!$. Alternatively, by treating the variable j as continuous, this set of linear equations reduces

to a simple convection-diffusion equation. Consequently, the width becomes diffusive, i.e. $\beta = \frac{1}{2}$.

4. Linear recursion relations

The LRR approach employs the exact uncovered fraction $S_1(t)$ in the first layer, provided by the KAJM solution (19) [6, 18, 30, 31]. Nucleation in the $(j+1)$th layer proceeds only on the already covered fraction of the jth layer, formed with rate $-dS_j/dt$. Subsequent covering proceeds as in the KAJM, so one can anticipate that nucleation events in the time interval $(\tau, \tau + d\tau)$ should provide contribution $S_1(t-\tau)[-\dot{S}_j(\tau)]d\tau$ to the exposed fraction $S_{j+1}(t) - S_j(t)$ in the $(j+1)$th layer. This leads to a recursion relation between adjacent layers:

$$S_{j+1}(t) = S_j(t) - \int_0^t d\tau\, S_1(t-\tau)\frac{dS_j(\tau)}{d\tau}. \tag{23}$$

The first layer coverage (19) can be recovered by setting the substrate coverage appropriately, $dS_0/dt = -\delta(t)$.

Although MFT and LRR are both recursive as every layer is coupled to the preceding layer, they differ in that the MFT equations are nonlinear, while the LRR equations are linear. Nevertheless, when $d \to 0$, both approximations are identical. Indeed, multiplying equation (23) by e^t and differentiating, one recovers the MFT equation (22).

Using the Laplace transform, analytical results for the growth velocity and the interface width have been established [31, 18, 19]. Hereafter, we give an alternative and simpler derivation which additionally provides the asymptotic behaviour of the coverage profile. In the long-time limit, it is reasonable to treat the layer number j as a continuous variable. Replacing the difference $S_{j+1} - S_j$ by a partial derivative, the recursive relations (23) become

$$\frac{\partial S}{\partial j} \cong -\int_0^t d\tau\, S_1(\tau)\frac{\partial S(j,t')}{\partial t'}\bigg|_{t'=t-\tau} \cong -\frac{1}{v_d}\frac{\partial S}{\partial t} + \frac{1}{2v_d^2}\,\frac{\Gamma\left(\frac{d+3}{d+1}\right)}{\Gamma^2\left(\frac{d+2}{d+1}\right)}\,\frac{\partial^2 S}{\partial t^2} \tag{24}$$

with v_d the growth velocity

$$v_d = \left(\frac{\Omega_d}{d+1}\right)^{\frac{1}{d+1}} \Big/ \Gamma\left(\frac{d+2}{d+1}\right). \tag{25}$$

The second line in (24) has been derived by expanding $S(j, t-\tau)$ in a Taylor series in τ, retaining only the two dominant terms of the expansion, and replacing the upper limit in the integral by ∞. The following growth velocities are found: $v_0 = 1$, $v_1 = 2/\sqrt{\pi} = 1.128\,38$, $v_2 = 1.137\,19$, and $v_d \to \sqrt{2\pi e/d}$ as $d \to \infty$. The velocity is almost constant for physical dimensions (it varies by less than 4% in the range $1 \leqslant d \leqslant 4$) indicating the weak dimension dependence of this approach.

Changing variables from (j, t) to $(j, \xi = j - v_d t)$ recasts equation (24) into a diffusion equation

$$\frac{\partial S}{\partial t} = D\frac{\partial^2 S}{\partial \xi^2}. \tag{26}$$

The constant $D = \frac{v_d}{2}\Gamma\left(\frac{d+3}{d+1}\right)/\Gamma^2\left(\frac{d+2}{d+1}\right)$ plays the role of a diffusion coefficient and controls the width of the interface. By obtaining equation (26), j was replaced by $v_d t$. This is clearly valid in the scaling limit, $j \to \infty$, $|\xi| \to \infty$, $j \sim \xi^2$. The initial profile of the uncovered

fraction, $S(j,0)$, is a step function: $S(j,0) = 0$ for $j \leqslant 0$ and $S(j,0) = 1$ for $j > 0$. Solving (26) subject to these initial conditions yields

$$S(j,t) = \tfrac{1}{2}\mathrm{erfc}(-z) \qquad z = \frac{\xi}{\sqrt{4Dt}} = \frac{j - v_d t}{\sqrt{4Dt}} \tag{27}$$

with $\mathrm{erfc}(z) = \frac{2}{\sqrt{\pi}} \int_z^\infty du\, \mathrm{e}^{-u^2}$ the error function [29]. While the two approximations generally differ in their asymptotic behaviour, they do agree in the extreme cases of $d = 0$ and $d = \infty$.

In summary, the LRR approach predicts a dimension-independent 'diffusive' width exponent $\beta = \frac{1}{2}$. The shape of the coverage profile is symmetric and Gaussian away from the front, $\sigma_\pm = 2$.

5. Comparison with simulations

To test the two approximations we simulated the PNG process. The simulation results presented below are for a one-dimensional chain of length $L = 10^4$ and represent a single realization. Our work is different from most previous numerical studies which simulated the PNG process on a lattice [24]. The 1D continuous PNG process is simple. The initial conditions consist of a flat substrate. Island nucleation corresponds to the creation of a kink–antikink pair, while island merger corresponds to a kink–antikink annihilation. A list of all distances between kink–antikink pairs moving towards each other is maintained throughout the simulation. These distances decrease linearly with time as the motion is ballistic. Thus, the first collision time is picked, and the annihilating pair is removed from the system. In parallel, kink–antikink pairs are nucleated with unit rate, and the distance list is updated accordingly. This simulation treats time and space as continuous variables. This allows a direct calculation of the growth velocity, which should vary from that obtained from lattice simulations. In contrast to previous simulations [18] of the first few layers, this calculation obtains the growth velocity to a much higher accuracy, as it is orders of magnitude larger in size as well as in temporal range.

The time dependence of the uncovered fraction for the first four layers is shown in figure 2. It is seen that the MFT and the LRR approaches provide upper and lower bounds, respectively, for the actual PNG coverage. Additionally, the MFT provides a better approximation for the uncovered fraction, $S_j(t)$. For early times, the height and width predicted by either approximations are relatively close to simulation results, as shown in figure 3. In fact, both approaches agree to the first significant order in time, as both equation (12) and equation (23) predict $S_j(t) = 1 - \frac{2^j}{(2j)!} t^{2j}$. The disagreement between the two is of the order t^{2j+2}. As the two approximations give upper and lower bounds for the PNG process, we conclude that this is the leading early time behaviour of $S_j(t)$.

However, both approximations become progressively worse at later times, owing to the fact that the asymptotic behaviour of the width is predicted incorrectly (see table 1). As the MFT predicts an asymptotically flat surface, both the roughness and width exponents vanish $\chi = \beta = 0$. Figure 4 shows that at least in one dimension, the PNG asymptotic behaviour belongs to the Kardar–Parisi–Zhang (KPZ) universality class [32]. This is consistent with the analytical result in 1D that gives $\chi = \frac{1}{2}$. As our simulations are continuous in space and time, they enable measurement of the surface growth velocity. Although in principle, there is no reason to expect that the surface growth velocity in an infinite and a finite system are equal, the numerical velocity $v_{\mathrm{noneq}} = 1.41 \pm 0.01$, which corresponds to (non-equilibrium) growth on an infinite substrate, is in very good agreement with the known

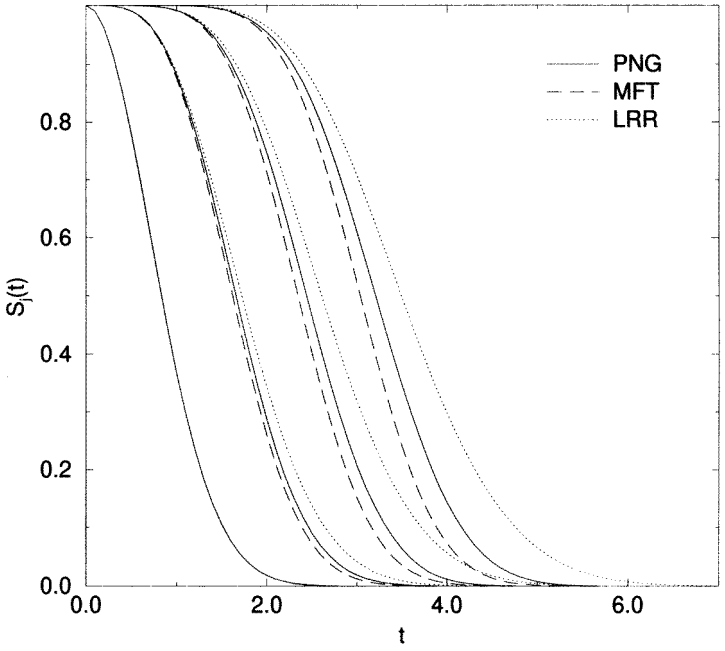

Figure 2. Uncovered fraction $S_j(t)$ versus t for $j = 1, 2, 3, 4$. MFT and LRR approaches give lower and upper bounds, respectively, for the uncovered fraction.

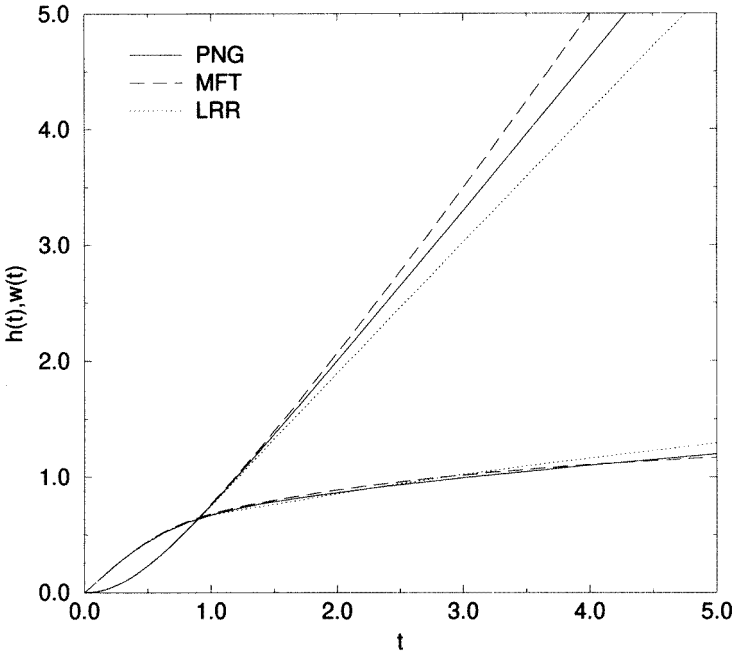

Figure 3. Short-time behaviour of the height $h(t)$ and the width $w(t)$. MFT is closer to the actual behaviour.

Table 1. Characteristics of the three approaches for the one-dimensional PNG model.

	MFT	PNG	LRR
v_1	1.757 35	1.41 ± 0.01	1.128 38
β	0	$\frac{1}{3}$	$\frac{1}{2}$
σ_+	1	$\frac{3}{2}$	2
σ_-	2	$\geqslant 2$	2

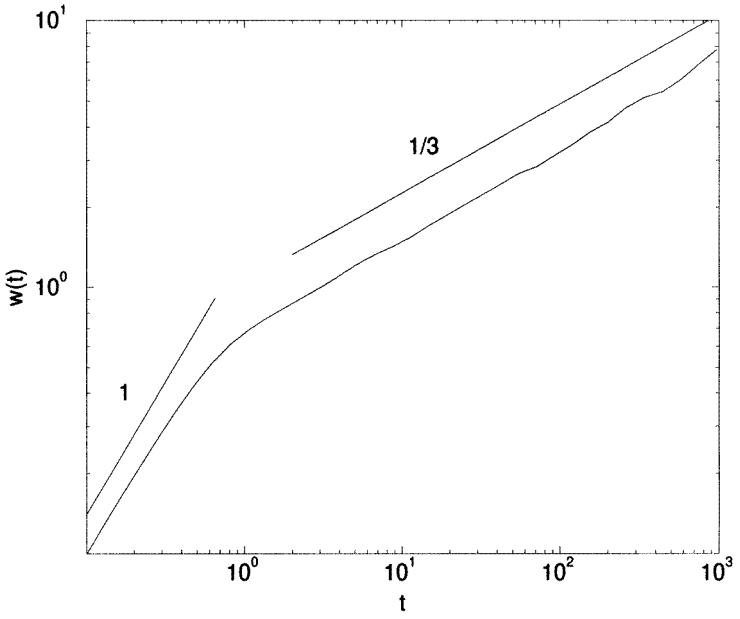

Figure 4. Long-time behaviour of the width. Early behaviour is linear and late behaviour is in the KPZ universality class $t^{1/3}$.

analytical equilibrium growth velocity $v_{\rm eq} = \sqrt{2}$ [20]. Numerical values for v, β and $\sigma_\pm$ are summarized in table 1. Two-dimensional simulations give a velocity $v_2 \approx 1.4$ [7] compared to the values $v_2 = 1.671$ (MFT) and $v_2 = 1.137$ (LRR). Furthermore, the exponent β decreases when the spatial dimension increases [3]. Thus the MFT improves for higher dimensions.

It is useful to note that the dynamical exponent for the 1D PNG is $z = \frac{3}{2}$, as it follows from the exponent relation $z = \chi/\beta$ together with $\chi = \frac{1}{2}$ and $\beta = \frac{1}{3}$. The finite size effects are negligible as long as $t \ll L^z$, so for the system size $L = 10^4$ we should guarantee that $t \ll 10^6$. The time range of our simulations, $t < 10^3$, is well within the above bound.

We also examined the extremal behaviour of $S_j(t)$ using the simulations. The scaling prediction (5) holds as the simulation data is consistent with the exponent value $\sigma_+ = 3/2$, in agreement with the KPZ behaviour [25]. Given that the PNG uncovered fraction is bounded by the two approximations, the parameters v, β, and therefore σ_+ are similarly bounded (see table 1.) Since the scaling argument involves the width, one cannot conclude *a priori* that the same holds for σ_-. Nevertheless, the exponent found in the simulation is relatively close to 2, or possibly slightly larger. In comparison, numerical studies of the KPZ equation suggest $\sigma_- \cong 2.5$ [33].

6. Conclusions

We have investigated a continuum model of multilayer growth, the PNG model. We confirmed that the LRR approximation implies dimension-independent growth exponents. Moreover, we found that the full coverage profile approaches a dimension-independent form, thus implying that this approximation effectively ignores interactions. It is therefore not surprising that the LRR gives the width exponent $\beta = \frac{1}{2}$ which is characteristic for non-interacting systems, such as the growth on a zero-dimensional substrate. We developed an alternative self-consistent mean-field approach which provides a better approximation for the uncovered fraction, and close estimates for the early time behaviour. Mathematically, the mean-field approach leads to an interesting system of directed higher order Toda equations. The mean-field approximation overestimates layer–layer interactions and implies a sharp interface, i.e. $\beta = 0$. Additionally, the two approximate approaches combine to give upper and lower bounds for statistical properties such as the coverage, the velocity, and the roughness.

The above MFT should allow computation of spacetime correlation functions and structure functions. Even more detailed analysis may be possible for 1D substrates. A bigger challenge is to solve the PNG process analytically. Such a solution will undoubtedly illuminate the theoretical understanding of non-equilibrium growth.

Acknowledgment

PLK acknowledges support from NSF and ARO.

References

[1] Krug J and Spohn H 1992 *Solids Far From Equilibrium* ed C Godrèche (Cambridge: Cambridge University Press)
[2] Meakin P 1993 *Phys. Rep.* **235** 191
[3] Halpin-Healy T and Zhang Y-C 1995 *Phys. Rep.* **254** 215
[4] Barabasi A-L and Stanley H E 1995 *Fractal Concepts in Surface Growth* (Cambridge: Cambridge University Press)
[5] Frank F C1974 *J. Cryst. Growth* **22** 233
[6] Kashchiev D 1977 *J. Cryst. Growth* **40** 29
[7] Gilmer G H 1980 *J. Cryst. Growth* **49** 465
[8] Keller A 1968 *Rep. Prog. Phys.* **31** 623
[9] Bassett D C 1995 *Principles of Polymer Morphology* (Cambridge: Cambridge University Press)
[10] Kolmogorov A N 1937 *Bull. Acad. Sci. USSR, Phys. Ser.* **1** 355
[11] Avrami M 1939 *J. Chem. Phys.* **7** 1103
Avrami M 1940 *J. Chem. Phys.* **8** 212
Avrami M 1941 *J. Chem. Phys.* **9** 177
[12] Johnson W A and Mehl P A 1939 *Trans. AIMME* **135** 416
[13] Sekimoto K 1986 *Physica* **135A** 328
[14] Sekimoto K 1991 *Int. J. Mod. Phys. B* **5** 1843
[15] Bradley R M and Strenski P N 1989 *Phys. Rev.* B **40** 8967
[16] Ben-Naim E and Krapivsky P L 1996 *Phys. Rev.* E **54** 3562
[17] Evans J W 1993 *Rev. Mod. Phys.* **65** 1281
[18] Bartelt M C and Evans J W 1993 *J. Phys. A: Math. Gen.* **26** 2743
[19] Newman T J and Volmer A 1996 *J. Phys. A: Math. Gen.* **29** 2285
[20] Bennett C H, Büttiker M, Landauer R and Thomas H 1981 *J. Stat. Phys.* **24** 419
[21] Goldenfeld N 1984 *J. Phys. A: Math. Gen.* **17** 2807
[22] van Saarlos W and Gilmer G H 1986 *Phys. Rev.* B **33** 4927
[23] Krug J and Spohn H 1989 *Europhys. Lett.* **8** 219

[24] Krug J, Meakin P and Halpin-Healy T 1992 *Phys. Rev.* A **45** 638
[25] Zhang Y C 1990 *Phys. Rev.* B **42** 4897
[26] Toda M 1967 *J. Phys. Soc. Japan* **22** 431
[27] Bramson M 1983 *Convergence of Solutions of the Kolmogorov Equation to Travelling Waves* (Providence, RI: American Mathematical Society)
[28] Murray J D 1989 *Mathematical Biology* (New York: Springer)
[29] Bender C M and Orszag S A 1984 *Advanced Mathematical Methods for Scientists and Engineers* (Singapore: McGraw-Hill)
[30] Armstrong R D and Harrison J A 1969 *J. Electrochem. Soc.* **116** 328
[31] Rangarajan S K 1973 *J. Electroanal. Chem.* **46** 125
[32] Kardar M, Parisi G and Zhang Y C 1986 *Phys. Rev. Lett.* **56** 889
[33] Kim J M, Bray A J and Moore M A 1991 *Phys. Rev.* A **44** 2345